Journal of Hazardous Materials 178 (2010) 180–186

Contents lists available at ScienceDirect

Journal of Hazardous Materials

journal homepage: www.elsevier.com/locate/jhazmat

Remarkable sensitivity for detection of bisphenol A on a gold electrode modified with nickel tetraamino phthalocyanine containing Ni–O–Ni bridges

Vongani Chauke, Fungisai Matemadombo, Tebello Nyokong*

Department of Chemistry, Rhodes University, Grahamstown 6140, South Africa

ARTICLE INFO

Article history:
Received 24 November 2009
Received in revised form 12 January 2010
Accepted 12 January 2010
Available online 20 January 2010

Keywords:
Bisphenol A
Nickel phthalocyanine
Electropolymerization
Gold
Electrocatalysis
Cyclic voltammetry

ABSTRACT

This work reports the electrocatalysis of bisphenol A on Ni(II) tetraamino metallophthalocyanine (NiTAPc) polymer modified gold electrode containing Ni–O–Ni bridges (represented as Ni(OH)TAPc). The Ni(II)TAPc films were electro-transformed in 0.1 mol L^{-1} NaOH aqueous solution to form 'O–Ni–O oxo bridges', forming *poly*-*n*-Ni(OH)TAPc (where *n* is the number of polymerising scans). *poly*-30-Ni(OH)TAPc, *poly*-50-Ni(OH)TAPc, *poly*-70-Ni(OH)TAPc and *poly*-90-Ni(OH)TAPc films were investigated. The polymeric films were characterised by electrochemical impedance spectroscopy and the charge transfer resistance (R_{CT}) values increased with film thickness. The best catalytic activity for the detection of bisphenol A was on *poly*-70-Ni(OH)TAPc. Electrode resistance to passivation improved with polymer thickness. The electrocatalytic behaviour of bisphenol A was compared to that of *p*-nitrophenol in terms of electrode passivation and regeneration. The latter was found to passivate the electrode less than the former. The *poly*-70-Ni(OH)TAPc modified electrode could reliably detect bisphenol A in a concentration range of 7×10^{-4} to 3×10^{-2} mol L^{-1} with a limit of detection of 3.68×10^{-9} mol L^{-1}. The sensitivity was 3.26×10^{-4} A mol^{-1} L cm^{-2}.

1. Introduction

The determination and oxidation of phenolic type compounds has been extensively studied due to their widespread presence in the atmosphere and in industrial waste waters [1,2]. Phenolic compounds are toxic to humans, animals and plants. Bisphenol A (BPA) in particular, which is a subject of this study, is among the most serious environmental contaminants.

BPA (Fig. 1(i)) is highly suspected to act as an endocrine disruptor [3–6]. BPA is commonly used as a monomer compound in the production of polycarbonate plastics and finds its way into rivers, lakes and oceans [7,8]. It is thus important that cheap effective ways of detecting BPA are developed.

Various methods have been employed in determining BPA and other phenolic compounds, these include: high performance liquid chromatography (HPLC) [8], gas chromatography coupled with mass spectrometry [8,9] and electrochemical methods [10–14].

Electrochemical methods are preferred since there is no need for extensive separation. The electrochemical oxidation of phenols readily occurs on bare electrodes; however, oxidation results in the formation of dimers which poison the electrode, thus decreasing the oxidation current [14]. To combat this problem, modified electrodes have been used; metallophthalocyanine (MPc) modified electrodes in particular have shown good electrocatalytic activity [14].

This work reports the electrocatalytic oxidation of bisphenol A on nickel tetraamino phthalocyanine (Ni(II)TAPc) (Fig. 1(iii)) modified electrode containing Ni–O–Ni bridges. It has been reported that when NiPc derivatives are transformed into the 'O–Ni–O oxo form', better catalytic activity is observed for detection of chlorophenols [14–16] and other analytes. Hence in this work, the NiTAPc species is transformed to the O–Ni–O form for BPA detection. BPA has been determined on cobalt phthalocyanine (CoPc) modified carbon paste electrode (CPE) [17] with a detection limit of 1.0×10^{-8} mol L^{-1} and a linear range of 8.75×10^{-8} to 1.25×10^{-5} mol L^{-1}. Even though CPEs have the advantage of renewable electrode surfaces, they suffer from the effects of the binding materials employed such as leaking and partial inhibition of the faradaic currents [18]. On the other hand, passivation of the solid electrodes by the products of phenol oxidation is a serious limitation [14]. It has been reported that when NiPc derivatives are transformed into the 'O–Ni–O oxo form', electrode fouling is decreased [12], hence the use of this species for electrode modification in this work. BPA oxidation occurred on bare CPE, with only a slight increase in currents in the presence of CoPc, hence showing only small catalytic activity [17]. Thus the use of gold electrode was influenced by the fact that there is no oxidation peak for BPA on bare Au, making detection using NiPc easier. Recently [19] bisphenol A has been analysed at a glassy carbon electrode which had been elaborately modified with

* Corresponding author at: P.O. Box 94, Grahamstown, South Africa.
Tel.: +27 46 6038260; fax: +27 46 6225109.
E-mail address: t.nyokong@ru.ac.za (T. Nyokong).

0304-3894/$ – see front matter © 2010 Elsevier B.V. All rights reserved.
doi:10.1016/j.jhazmat.2010.01.061

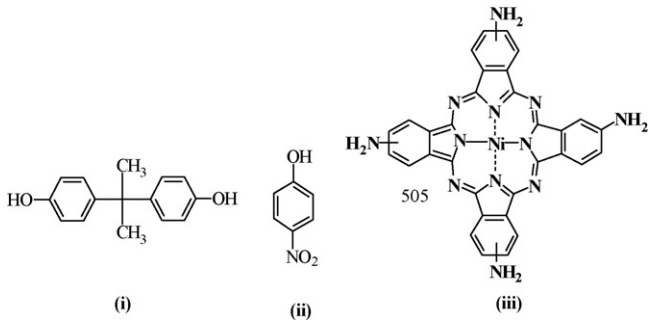

Fig. 1. Molecular structure of bisphenol A (i), *p*-nitrophenol (ii) and nickel tetraamino phthalocyanine (iii).

a multi-walled carbon nanotubes–gold nanoparticles hybrid film, with a linear range of 2.0×10^{-8} to 2×10^{-5} mol L^{-1} and a limit of detection of 7.5 nmol L^{-1}. The current work combines the catalytic activity of the NiTAPc and reduced passivation in the presence of O–Ni–O bridges.

The oxidation of BPA on nickel tetraamino phthalocyanine (Ni(II)TAPc) modified electrode containing Ni–O–Ni bridges, is compared with that of another phenol, namely *p*-nitrophenol (PNP) (Fig. 1(ii)) in terms of electrode passivation. PNP is used as an intermediate in the synthesis of paracetamol and mainly in the production of herbicides, pesticides, dyes and explosives [3,20]. Although its mode of action in the human body and animals is not entirely known, reports have shown that it may cause inflammation of eyes, skin and respiratory tract [20].

2. Experimental

2.1. Materials

N′-Dimethylformamide (DMF) from Aldrich was freshly distilled. Tetrabutylammonium tetrafluoroborate ($TBABF_4$) (Aldrich) was used as the electrolyte for electrochemical experiments. Bisphenol A (BPA) was purchased from Sigma–Aldrich. *p*-Nitrophenol was purchased from the British drug house (BDH). The syntheses of NiTAPc have been reported before [21].

2.2. Electrochemical apparatus and methods

Cyclic voltammetry (CV) experiments were performed using Autolab Potentiostat/Galvanostat model 263A (Princeton Applied research) driven by the Electrochemistry Powersuit software, using a conventional three-electrode system. Faradaic impedance measurements were performed with Autolab FRA equipment using a 10 mV root mean square (rms) sinusoidal modulation. The working electrodes were either bare or Au (1.6 mm diameter) modified with Ni(II)TAPc. Respectively, silver–silver chloride (Ag|AgCl) and platinum wire were used as pseudo-reference and counter electrodes. All the solutions were de-aerated by bubbling argon preceding the experiments and the argon atmosphere was maintained throughout the experiments. The pH 7 and 12 phosphate buffer solutions were prepared from KH_2PO_4 and Na_2HPO_4, and NaOH was used to adjust the pH. A stock solution of 1×10^{-2} mol L^{-1} bisphenol A or *p*-nitrophenol (PNP) was prepared in a mixture of deionised water/acetonitrile (60:30, v/v). This solvent mixture was employed due to the lack of solubility of BPA or PNP in water alone.

Samples for BPA practical application were obtained from a local food market. Two types of plastic products were used: microwave plastic (taken from a meat package) and a soft drink plastic bottle. Both plastics (microwave plastic and soft drink bottle) were washed thoroughly with water and soap to remove animal fat and blood-stains or soft drink leftovers. The microwave plastic was added to water and exposed to microwaves at high power for 5 min [17]. This was repeated three times on different days. The soft drink bottle was cut into small pieces and treated with hot boiling water. The treatment with hot water was repeated three times. To determine the concentration of BPA, the standard addition method was used.

The modification of the working Au electrode was achieved by electropolymerization of Ni(II)TAPc by repetitive cycling at a constant scan rate of 0.1 V s^{-1} in a potential range of −0.5 to 1.0 V to form *poly*-NiTAPc.

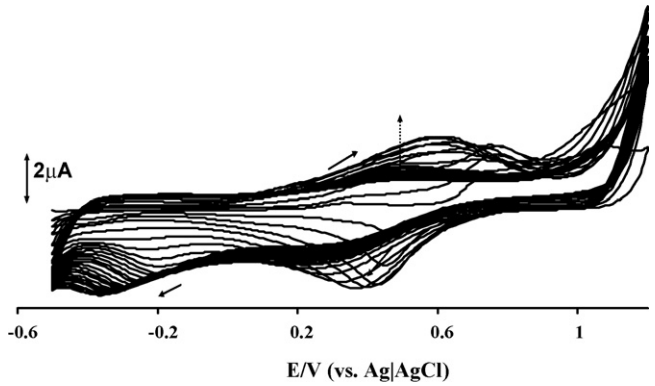

Fig. 2. Repetitive cyclic voltammogram of 1×10^{-3} mol L^{-1} NiTAPc in DMF containing 0.1 mol L^{-1} $TBABF_4$ at the gold electrode. Scan rate = 100 mV s^{-1}.

3. Results and discussion

3.1. Electrode modification using Ni(II)TAPc

The modification of the working Au electrode was achieved via electropolymerization of NiTAPc in DMF by repetitive cycling at a constant scan rate of 0.1 V s^{-1} to form *poly*-NiTAPc. The electropolymerization of CoTAPc and MnTAPc on glassy carbon electrodes is now well known [22,23]. The formation of self-assembled monolayers (SAMs) of CoTAPc, CuTAPc and FeTAPc on Au and Ag has been reported [24]. The formation of SAM is not expected to be significant during the time used for electropolymerization. SAM formation takes hours for significant coverage. Also the Au oxide and stripping peaks were not observed under the conditions (organic media) of the electropolymerization process.

Fig. 2 shows a series of CVs (20 scans) during electropolymerization of Ni(II)TAPc. The number of CV scans of 30 and 50 were also tried, but as has been observed before [13], the polymer film tends to lose conductivity with an increasing number of scans. Thus, the formation of O–Ni–O oxo bridges was based on the optimum number of scans of 20. Also, the main aim was to form O–Ni–O oxo bridges for the catalytic oxidation of BPA. It is well known that repetitive cyclic voltammetry scanning of amino substituted MTAPc complexes results in polymer formation of the MPc onto the electrode surface [22–26]. This is as a result of the formation of radicals on oxidizing the amino substituents [25], whereby the formed radicals attack the vulnerable phenyl rings of neighbouring molecules thus forming a polymer [25]. The cyclic voltammogram (CV) evolution shown in Fig. 2 is similar to that reported in the literature [25]. A general increase in currents together with the formation of new peaks was observed. The polymer formed was clearly noticeable on the surface of the electrode as a dark green surface. *poly*-NiTAPc will be used to represent the Ni(II)TAPc polymer on Au electrode surface. A slight shift on the positive potentials with increase in scan number was observed. This is indicative of an increase in electrical resistance of the polymer film and thus over-potential is needed to overcome resistance [27].

Table 1
EIS parameters and surface coverage values for *poly*-NiTAPc films, and recovery values for detection of BPA in pH 12 buffer.

Electrode	Surface coverage (Γ) mol cm^{-2} (MPc)	% Recovery for BPA	% Recovery for PNP	R_{CT} ($\times 10^{-3}$ Ω)	R_S (kΩ)	C_{dl} (μF)
Bare	0.0			13.2	0.16	0.32
poly-30-Ni(OH)NiTAPc-Au	1.79×10^{-10}	16	76	9.3	0.19	0.37
poly-50-Ni(OH)NiTAPc-Au	2.20×10^{-10}	25	91	5.7	0.19	0.53
poly-70-Ni(OH)NiTAPc-Au	5.46×10^{-10}	61	91	4.3	0.18	0.82
poly-90-Ni(OH)NiTAPc-Au	1.11×10^{-10}	72	65	4.5	0.15	0.82

Following the electropolymerization of Ni(II)TAPc, transformation of the *poly*-NiTAPc into 'O–Ni–O oxo bridges' was done by cycling repetitively in 0.1 mol L^{-1} solution of NaOH between −0.2 and 1.0 V. Fig. 3 shows the formation and increase of both the anodic and cathodic peaks between −0.2 and +0.5 V. These peaks are documented as the Ni^{III}/Ni^{II} redox process and are similar to literature [16,28]. The insert in Fig. 3 shows a cyclic voltammogram of the transformed polymer in pH 12 phosphate buffer, which is the pH employed for the detection of BPA. There is only a small shift to more positive potential values in pH 12 compared to in 0.1 mol L^{-1} NaOH. The cyclic voltammetry peaks between −0.2 and +0.5 V can be explained by the formation of 'O–Ni–O oxo bridges' in alkaline aqueous solutions and are indicative of transformation of the *poly*-NiTAPc into O–Ni–O oxo bridges [27–30]. The modified electrode will now be represented as *poly*-Ni(OH)TAPc–Au. Although the mechanism of transformation is not fully known, it has been suggested [30,31] that the transformation is initiated by the electrooxidation of the OH^- in the electrolyte solution to the hydroxyl radical ($OH^\bullet$). The high current observed between 0.7 and 1.0 V has been attributed to the electrooxidation of the OH^- [32]. The $OH^\bullet$ radicals assist with the insertion of the oxygen atom (O) between the NiPcs. With increase in scanning, more $OH^\bullet$ radicals are generated thus leading to the interlinking of the Ni atoms to form 'O–Ni–O oxo bridges'. There are no peaks due to Au alone at the pH employed.

3.2. Electrochemical behaviour of the electrodes and effect of film thickness

The thickness of the films is governed by the number of scans during polymerisation. The more the number of scans, the thicker the film. Ideally a thicker film should give better catalytic behaviour than a thinner one. This is expected because of the availability of more catalytic sites. However, it has been shown before that the accessibility to the redox centres within the electropolymerised films is limited to the external layers [32].

Fig. 4 shows the cyclic voltammograms of (i) Au electrode, (ii) *poly*-30-Ni(OH)NiTAPc, (iii) *poly*-50-Ni(OH)NiTAPc, (iv) *poly*-70-Ni(OH)NiTAPc, (v) *poly*-90-Ni(OH)NiTAPc in 1×10^{-3} mol L^{-1} $K_3[Fe(CN)_6]$ containing 0.1 mol L^{-1} KCl. The bare electrode in Fig. 4(i) shows a redox couple at a half-wave potential ($E_{1/2}$) of 65 mV and an anodic to cathodic peak separation (ΔE) of 130 mV. Fig. 4(ii)–(v) shows reversible cyclic voltammograms with $E_{1/2}$ values decreasing with increasing polymer thickness from $E_{1/2}$ = 135 mV for *poly*-30-Ni(OH)NiTAPc, 130 mV for *poly*-50-Ni(OH)NiTAPc, 120 mV for *poly*-70-Ni(OH)NiTAPc and 115 mV for *poly*-90-Ni(OH)NiTAPc. The decrease in ΔE values was also observed with polymer thickness (with the exception of *poly*-90-Ni(OH)NiTAPc) as follows: 120 mV for *poly*-30-Ni(OH)NiTAPc, 80 mV for *poly*-50-Ni(OH)NiTAPc, 60 mV for *poly*-70-Ni(OH)NiTAPc and 70 mV for *poly*-90-Ni(OH)NiTAPc. This order suggests improved kinetics with increase in polymer thickness. The peak current also increased compared to bare Au electrode in Fig. 4.

In order to estimate the surface concentration of the complexes on gold electrodes, the effective surface areas of the gold electrodes were first determined using the Randles–Sevcik equation [33], Eq. (1), and Fig. 4 for the cyclic voltammogram of $[Fe(CN)_6]^{3-}$ in 1×10^{-3} mol L^{-1} KCl:

$$I_{pa} = (2.69 \times 10^5) n^{3/2} D^{1/2} \upsilon^{1/2} AC \quad (1)$$

where n is the number of electrons transferred (n = 1), D is the diffusion coefficient of $[Fe(CN)_6]^{3-}$ (7.6×10^{-6} cm^2 s^{-1} [34]), υ is the scan rate, A is the effective surface area, C is the bulk concentration of $[Fe(CN)_6]^{3-}$ (1×10^{-3} mol L^{-1}).

The surface coverages ($\Gamma_{polyMTAPc}$) of polymer modified electrodes were estimated by integrating the charge under the reduction peak in Fig. 3(insert), using Eq. (2).

$$\Gamma_{polyMTAPc} = \frac{Q}{nFA} \quad (2)$$

where Q (C) is the charge under the metal oxidation peak, n (=1) is the number of electrons, A is the effective area of the electrode (calculated from Eq. (1)) and F is Faraday's constant (95,485 C mol^{-1}). Using the effective area of the electrodes, the calculated surface coverage values for the various polymers are listed in Table 1. The determined values range from 1.11×10^{-10} to 5.46×10^{-10} mol cm^{-2}. These values are in the range for monolayer coverage in MPc complexes [35].

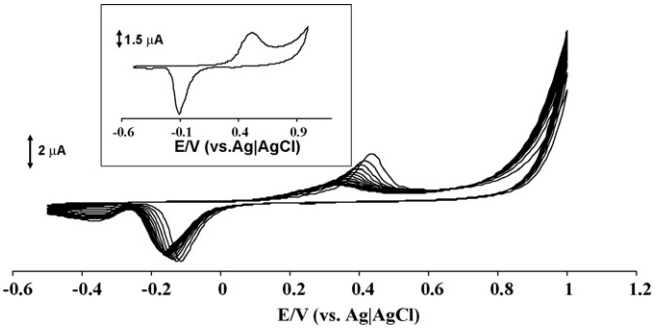

Fig. 3. Repetitive cyclic voltammograms of *poly*-NiTAPc in 0.1 mol L^{-1} NaOH. Insert is the polymer in buffer. Scan rate = 100 mV s^{-1}.

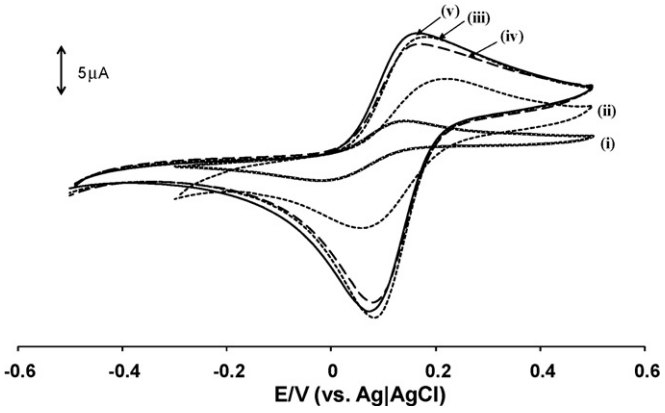

Fig. 4. Cyclic voltammograms of (i) Au bare electrode, (ii) *poly*-30-Ni(OH)NiTAPc, (iii) *poly*-50-Ni(OH)NiTAPc, (iv) *poly*-70-Ni(OH)NiTAPc, (v) *poly*-90-Ni(OH)NiTAPc in 1×10^{-3} mol L^{-1} $K_3[Fe(CN)_6]$ containing 0.1 mol L^{-1} KCl. Scan rate = 100 mV s^{-1}.

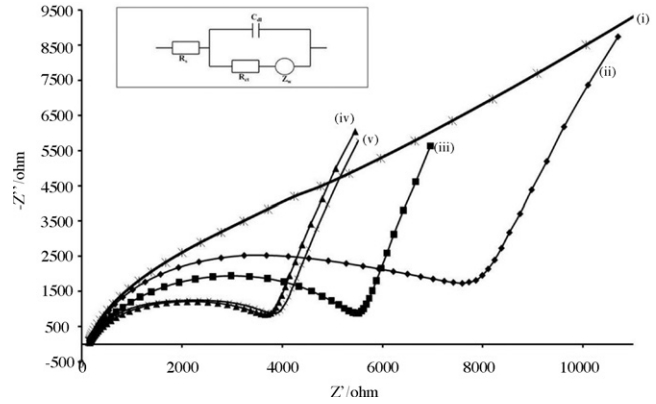

Fig. 5. Nyquist plots of electrodes of this work recorded in 1×10^{-3} mol L^{-1} $[Fe(CN)_6]^{3-/4-}$ in 0.1 mol L^{-1} KCl: (i) bare, (ii) *poly*-30-Ni(OH)NiTAPc, (iii) *poly*-50-Ni(OH)NiTAPc, (iv) *poly*-70-Ni(OH)NiTAPc, (v) *poly*-90-Ni(OH)NiTAPc modified Au electrodes. The insert shows the Randles equivalent circuit of the electrodes.

Electrochemical impedance spectroscopy (EIS) was employed for further characterization of the modified electrodes. The Nyquist plot ($-Z''$ vs. Z') was fitted and analysed using the Randles equivalent circuit (Fig. 5(insert)) which takes into consideration the diffusion and kinetic control parameters [36–38]. The Randles equivalent circuit used for fitting impedance data consisted of the solution or electrolyte resistance (R_S) connected in series to the parallel combination of the capacitance and charge transfer resistance (R_{CT}) in series with Warburg impedance (Z_W).

Fig. 5 shows the Nyquist plots for (i) bare and (ii) *poly*-30-Ni(OH)NiTAPc, (iii) *poly*-50-Ni(OH)NiTAPc, (iv) *poly*-70-Ni(OH)NiTAPc, and (v) *poly*-90-Ni(OH)NiTAPc modified Au electrodes recorded in 1×10^{-3} mol L^{-1} $[Fe(CN)_6]^{3-/4-}$ in 0.1 mol L^{-1} KCl. The bare electrode shows an almost straight line. The Nyquist plots of all the modified electrodes (Fig. 5(ii)–(v)) resemble a semicircle pattern (due to barrier to the interfacial electron-transfer) followed by a straight line in the low frequency region (the Warburg line).

The charge transfer resistance (R_{CT}) (Table 1) decreases with film thickness, except for *poly*-70-Ni(OH)NiTAPc and *poly*-90-Ni(OH)NiTAPc, whose values are almost the same. The behaviour of *poly*-70-Ni(OH)NiTAPc and *poly*-90-Ni(OH)NiTAPc implies that film thickness in this case does not necessarily mean less charge transfer resistance or better catalytic activity as reported before [31]. The general decrease in R_{CT} values with film thickness could be attributed to the catalytic nature of the surface confined polymer films as has been observed before [39,40]. This behaviour may be a result of decreased electrical resistance to mass transport through the film thickness. The decreases in R_{CT} values confirm the cyclic voltammetry results which showed improvement in ferrocene peak separation with film thickness.

The R_S values (Table 1) between the different polymers on Au electrodes were not significantly different (0.15–0.19 kΩ). The polymers on the electrode surfaces are not expected to change the solution resistance significantly, hence this was expected. The C_{dl} values were different, with *poly*-70-Ni(OH)NiTAPc showing the highest value of 0.82 μF and bare gold electrode showing the smallest value of 0.32 μF. The differences show the different conducting abilities of the different films.

3.3. Electrocatalysis of bisphenol A using poly-Ni(OH)TAPc

Fig. 6a shows the cyclic voltammograms recorded in 2×10^{-3} mol L^{-1} BPA in pH 12 phosphate buffer on *poly*-*n*-Ni(OH)NiTAPc (containing O–Ni–O bridges, where *n* is the number of polymerization scans). From Fig. 6a, the modified electrodes showed peaks for BPA oxidation, showing that the NiPc species catalyses the oxidation. There were no BPA peaks on bare Au electrode. The peak for the oxidation of BPA was observed at 0.45 V (vs. Ag|AgCl) which is 0.41 V vs. saturated calomel electrode (SCE) (using a −0.045 V correction factor [41]). This value is slightly less positive than the value of 0.45 V vs. SCE obtained on CoPc-CPE [17]. However, since no oxidation peak for BPA is observed on bare Au electrode in the current work, the detection of this species is hence more convenient compared to its detection on CPE. The return peak near 0.28 V in Fig. 6a is attributed to the reduction of the oxidation products of BPA.

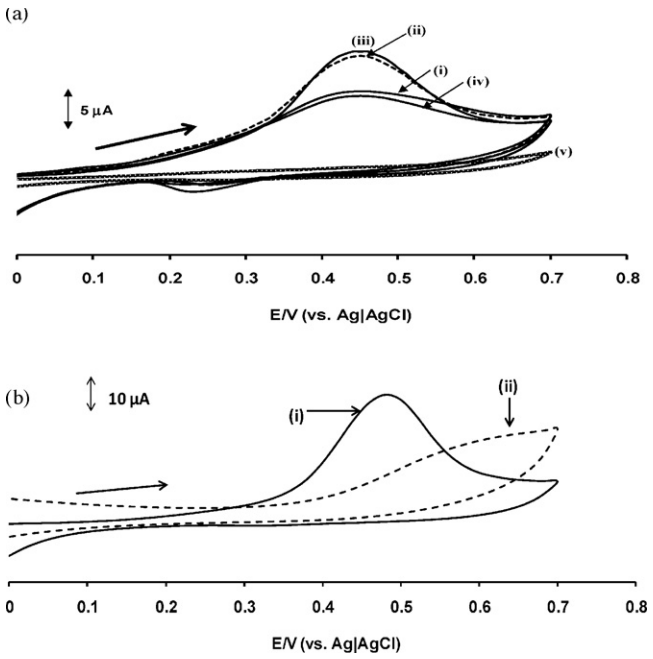

Fig. 6. Cyclic voltammograms recorded in 2×10^{-3} mol L^{-1} BPA in pH 12 phosphate buffer: (a) (i) *poly*-30-Ni(OH)NiTAPc, (ii) *poly*-50-Ni(OH)NiTAPc, (iii) *poly*-70-Ni(OH)NiTAPc, (iv) *poly*-90-Ni(OH)NiTAPc, and (v) bare gold electrode; (b) of *poly*-Ni(OH)TAPc (i) and *poly*-NiTAPc (ii) modified electrodes. Scan rate = 100 mV s^{-1}.

It is expected that a thicker film should be the most sensitive (due to the availability of more catalytic sites). However, this was not the case in this study. It has also been shown before that catalysis by polymerised films is only limited to external layers [32]. For BPA oxidation reactions *poly*-70-Ni(OH)NiTAPc was the most sensitive towards the oxidation of BPA of all the polymers. This could be explained by the fact that the R_{CT} value of *poly*-70-Ni(OH)NiTAPc showed less resistance, making the polymer more catalytic. The largest surface coverage was for *poly*-70-Ni(OH)NiTAPc.

Fig. 6b demonstrates that *poly*-Ni(OH)TAPc modified electrode (i) shows good catalytic activity to bisphenol A compared to *poly*-NiTAPc modified electrode (ii). This is judged by the fact that *poly*-Ni(OH)TAPc displays less positive potential for bisphenol A detection (0.45 V vs. Ag|AgCl) compared to *poly*-NiTAPc which detected bisphenol A at ~0.62 V vs. Ag|AgCl (Fig. 6b). Also, a higher peak current in the detection of bisphenol A was obtained on the *poly*-Ni(OH)TAPc (i) relative to *poly*-NiTAPc (ii) (Fig. 6b). Furthermore, a sharper and better defined bisphenol A detection peak was displayed by the *poly*-Ni(OH)TAPc (i) relative to *poly*-NiTAPc (ii) (Fig. 6b).

Fig. 7 shows the cyclic voltammograms of 2×10^{-3} mol L^{-1} PNP in pH 12 phosphate buffer on *poly*-Ni(OH)TAPc (containing O–Ni–O bridges). There was a significant potential shift (peak at ~0.76 V) for

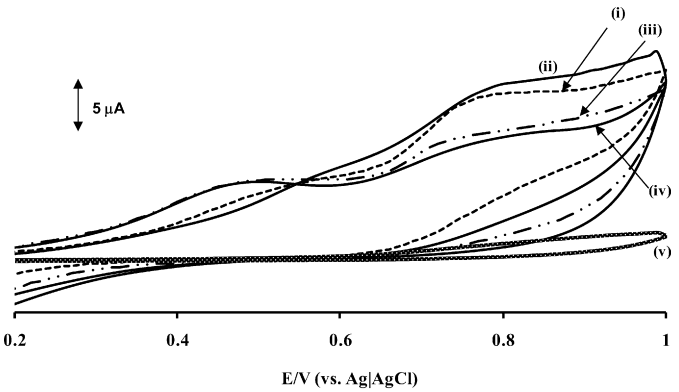

Fig. 7. Cyclic voltammograms of 2×10^{-3} mol L^{-1} PNP in pH 12 phosphate buffer: (i) *poly*-30-Ni(OH)TAPc, (ii) *poly*-50-Ni(OH)TAPc, (iii) *poly*-70-Ni(OH)TAPc, (iv) *poly*-90-Ni(OH)TAPc and (v) bare gold electrode. Scan rate = 100 mV s^{-1}.

the catalytic oxidation of PNP compared to BPA (peak at 0.45 V). The peak observed at ~0.5 V for PNP catalysis by *poly*-30-Ni(OH)TAPc and *poly*-90-Ni(OH)TAPc is most likely due to Ni^{III}/Ni^{II} in comparison with Fig. 3. *poly*-30-Ni(OH)TAPc and *poly*-50-Ni(OH)TAPc were the most sensitive towards the oxidation of PNP (Fig. 7) while, as stated above, *poly*-70-Ni(OH)TAPc was the most sensitive for BPA. There was a decrease in current for *poly*-70-Ni(OH)TAPc for BPA and after *poly*-50-Ni(OH)TAPc for PNP.

The mechanism for the oxidation of BPA is expected to be similar to that proposed for its oxidation on CoPc-CPE [17] (Scheme 1) but catalysed by $Ni^{III}Pc/Ni^{II}Pc$ instead of the corresponding CoPc couple. Catalysis was carried out in basic media where BPA deprotonates (step 1). The catalytic oxidation occurs at potentials where Ni(III) exits for *poly*-Ni(OH)TAPc, hence it catalyses oxidation of BPA to form radicals (step 3) which subsequently dimerise to form polymers as indicated in steps 4–5. For *poly*-NiTAPc, only ring based processes will be involved since, without transformation to Ni–O–Ni bridges, NiPc complexes do not show the Ni(III)/Ni(II) couple.

Fig. 8 shows the linear variation of the electrocatalytic currents plateaus (steady-state currents) with BPA concentrations in the range of 7×10^{-4} to 3×10^{-2} mol L^{-1} for Au *poly*-70-Ni(OH)NiTAPc. A linear coefficient above 0.998 was obtained. The calculated sensitivity (obtained from the slope of the linear plot) was 3.26×10^{-4} A mol^{-1} L cm^{-2}. The limit of detection (LoD) was calculated according to literature [42], using the 3δ/slope ratio notation (where δ is the standard deviation of the plot in Fig. 8), and found to be 3.68×10^{-9} mol L^{-1} for BPA on *poly*-70-Ni(OH)NiTAPc. This value is better than that

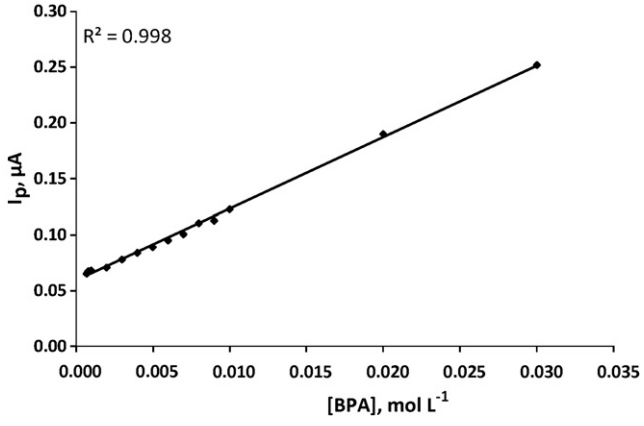

Fig. 8. Calibration curves for BPA detection by *poly*-70-Ni(OH)NiTAPc (pH = 12).

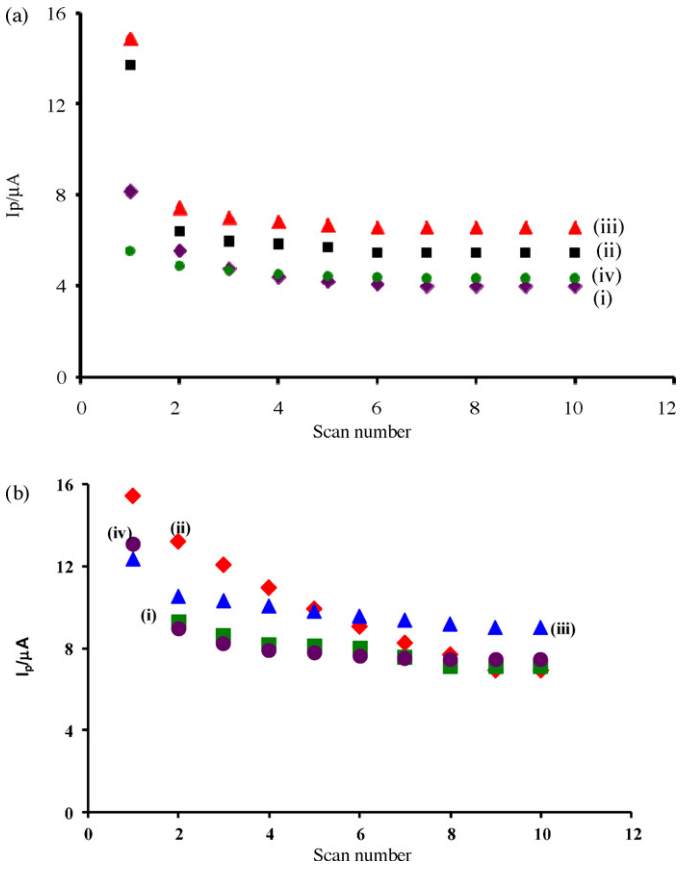

Fig. 9. The variation of peak currents with scan number for the voltammetric responses in 2×10^{-3} mol L^{-1} (a) BPA and (b) PNP at (i) *poly*-30-Ni(OH)NiTAPc, (ii) *poly*-50-Ni(OH)NiTAPc, (iii) *poly*-70-Ni(OH)NiTAPc, and (iv) *poly*-90-Ni(OH)NiTAPc modified gold electrode.

reported for CoPc-CPE (LoD = 1.0×10^{-8} mol L^{-1}) [17] and carbon electrode which had been modified with a multi-walled carbon nanotubes–gold nanoparticles hybrid film [19]. Thus the *poly*-Ni(OH)NiTAPc on gold shows excellent sensitivity for BPA.

BPA concentrations were calculated in the two types of plastics that were obtained from a local food store for practical analysis using *poly*-70-Ni(OH)NiTAPc which was the most sensitive towards the oxidation of BPA. This was performed to determine the possible potential of the modified gold electrodes in the detection of BPA in real sample applications. A standard addition method was employed, where it was discovered that the microwave oven plastic had more BPA concentration (2.55 μM) than the soft drink bottle which had a BPA concentration of 0.585 μM. Values in the μM range were obtained for similar samples [17].

3.4. Electrode passivation

Phenolic type compounds are disreputable for fouling electrode surfaces. This is due to the fact that when they are oxidized, phenol polymerization and hydroquinone formation take place [15,16] and thus block the electrode surface. Fig. 9 shows a decrease in current responses of BPA or PNP with cyclic voltammetry scan number. There is a decrease in current after the first scan followed by stabilization of the current. The electrodes could be partially regenerated by rinsing in pH 7.4 buffer, with percentage recoveries listed in Table 1. It was also observed that percentage recovery values increased with increase in polymer thickness, with the exception of *poly*-90-Ni(OH)NiTAPc for PNP. The percentage recovery values in Table 1 show that it was easier to regenerate surfaces with PNP

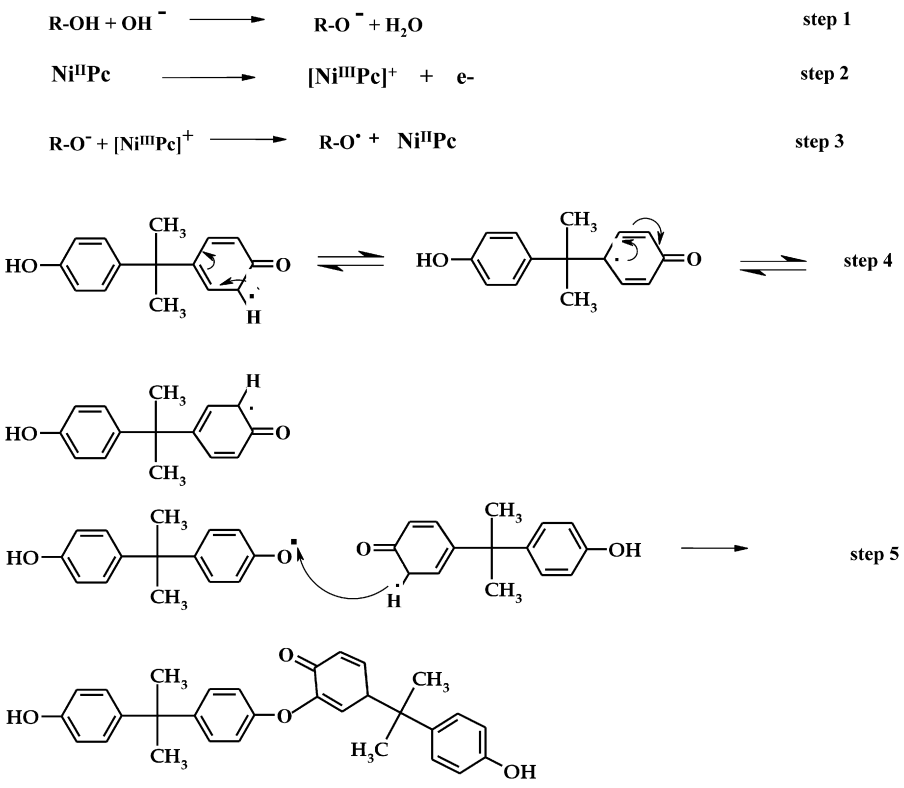

Scheme 1. Proposed reaction mechanism for the electrooxidation of BPA, where R (in steps 1 and 3) represents the rest of the BPA molecule.

oxidation products than those of BPA, the recovery values of the latter range from 16 to 72% for BPA and 65 to 91% for PNP.

4. Conclusion

The electrooxidation of BPA and PNP in pH 12 buffer by different *poly*-NiTAPc of different thicknesses was investigated. It was also demonstrated that thicker films do not necessarily give better catalysis. *poly*-70-Ni(OH)NiTAPc was the most sensitive for the electrocatalysis of BPA. The stability of the electrodes increased with polymer thickness. The *poly*-70-Ni(OH)TAPc modified electrode (which showed the largest sensitivity) could reliably detect bisphenol A in a concentration range of 7×10^{-4} to 3×10^{-2} mol L^{-1} with a limit of detection of 3.68×10^{-9} mol L^{-1}. The sensitivity was 3.26×10^{-4} A mol^{-1} L cm^{-2}. BPA passivates the electrode to a larger extent than PNP.

Acknowledgements

This work was supported by the Department of Science and Technology (DST) and National Research Foundation (NRF), South Africa through DST/NRF South African Research Chairs Initiative for Professor of Medicinal Chemistry and Nanotechnology as well as Rhodes University.

References

[1] K. Rajeshwar, J.G. Ibáñez, Environmental Electrochemistry: Fundamentals and Applications in Pollution Abatement, Academic Press, New York, 1997.
[2] E. Rudd, B.E. Conway, in: T.L. Rouge, O. Murphy (Eds.), Proceedings of Electrochemical Society Symposium on Water Purification by Photocatalytic, Photoelectrochemical Procedures and Electrochemical Procedures, The Electrochemical Society, Pennington, NJ, 1994, p. 94.
[3] Agency for Toxic Substances and Disease Registry (ATSDR), Toxicological Profile for Nitrophenols (Draft), Public Health Service, U.S. Department of Health and Human Services, Atlanta, GA, 1990.
[4] C. Sonnenschein, A.M. Soto, An updated review of environmental estrogen and androgen mimics and antagonists, J. Steroid Biochem. Mol. Biol. 65 (1998) 143–150.
[5] D. Crain, M. Eriksen, T. Iguchi, S. Jobling, H. Laufer, G. LeBlanc, L. Guillett, An ecological assessment of bisphenol-A: evidence from comparative biology, Reprod. Toxicol. 24 (2) (2007) 224–239.
[6] J. Oehlmann, M. Oetken, U. Schulte-Oehlmann, A critical evaluation of the environmental risk assessment for plasticizers in the freshwater environment in Europe, with special emphasis on bisphenol-A and endocrine disruption, Environ. Res. 108 (2) (2008) 140–149.
[7] A.V. Krishnan, P. Stathis, S.F. Permuth, L. Tokes, D. Feldman, Bisphenol-A: an estrogenic substance is released from polycarbonate flasks during autoclaving, Endocrinology 132 (1993) 2279–2286.
[8] J.A. Brotons, M.F. Olea-Serrana, M. Villalobos, V. Pedraza, N. Olea, Xenoestrogens released from lacquer coatings in food cans, Environ. Health Perspect. 103 (1995) 608–612.
[9] A. Gonzalez-Casado, N. Navas, M. Del-Olmo, J.L. Vilchez, Determination of bisphenol A in water by microliquid-liquid extraction followed by silylation and GC–MS, J. Chromatogr. Sci. 36 (1998) 565–569.
[10] Y. Wen, B.-S. Zhou, Y. Xu, S.-W. Jin, Y.-Q. Feng, Analysis of estrogens in environmental waters using polymer monolith in-polyether ether ketone tube solid-phase microextraction combined with high-performance liquid chromatography, J. Chromatogr. A 1133 (2006) 21–28.
[11] G. Gatidou, N.S. Thomaidis, A.S. Stasinakis, T.D. Lekkas, Simultaneous determination of the endocrine disrupting compounds nonylphenol, nonylphenol ethoxylates, triclosan and bisphenol A in wastewater and sewage sludge by gas chromatography–mass spectrometry, J. Chromatogr. A 1138 (2007) 32–41.
[12] C. Borras, T. Laredo, B.R. Scharifker, Competitive electrochemical oxidation of p-chlorophenol and p-nitrophenol on Bi-doped PbO_2, Electrochim. Acta 48 (2003) 2775–2780.
[13] J. Obirai, F. Bedioui, T. Nyokong, Electro-oxidation of phenol and its derivatives on *poly*-Ni(OH)TPhPyPc modified vitreous carbon electrodes, J. Electroanal. Chem. 576 (2005) 323–332.
[14] T. Nyokong, in: J.H. Zagal, F. Bedioui, J.-P. Dodelet (Eds.), N_4-Macrocyclic Metal Complexes, Springer, New York, 2006.
[15] B. Agboola, T. Nyokong, Electrocatalytic oxidation of chlorophenols by electropolymerised nickel(II) tetrakis benzylmercapto and dodecylmercapto metallophthalocyanines complexes on gold electrodes, Electrochim. Acta 52 (2007) 5039–5045.
[16] B.O. Agboola, K.I. Ozoemena, T. Nyokong, Electrochemical properties of benzylmercapto and dodecylmercapto tetra substituted nickel phthalocyanine complexes: electrocatalytic oxidation of nitrite, Electrochim. Acta 51 (2006) 6470–6478.
[17] H.-S. Yin, Y.-L. Zhou, S.-Y. Ai, Preparation and characteristic of cobalt phthalocyanine modified carbon paste electrode for bisphenol A detection, J. Electroanal. Chem. 626 (2009) 80–88.
[18] W.T.L. da Silva, C. Thobie-Gautier, M.O.O. Rezende, N. El Mu, Electrochemical behavior of Cu(II) on carbon paste electrode modified by humic acid, cyclic voltammetry study, Electroanalysis 14 (2002) 71–77.

[19] X. Tu, L. Yan, X. Luo, S. Luo, Q. Xie, Electroanalysis of bisphenol A at a multi-walled carbon nanotubes-gold nanoparticles modified glassy carbon electrode, Electroanalysis 21 (2009) 2491–2494.
[20] F. Eyer, V. Meischner, D. Kiderlen, H. Thiermann, F. Worek, M. Haberkorn, N. Felgenhauer, T. Zilker, P. Eyer, Human parathion poisoning: a toxicokinetic analysis, Toxicol. Rev. 22 (2003) 143–163.
[21] B.N. Achar, G.M. Fohlen, J. Keshavayya, Synthesis and structural studies of metal(II) 2,9,16,23-phthalocyanine tetraamines, Polyhedron 6 (1987) 1463–1467.
[22] E. Trollund, P. Ardiles, M.J. Aguirre, S.R. Biaggio, R.C. Rocha-Filho, Spectroelectrochemical and electrical characterization of poly(cobalt-tetraaminophthalocyanine)-modified electrodes: electrocatalytic oxidation of hydrazine, Polyhedron 19 (2002) 2303–2312.
[23] J. Obirai, T. Nyokong, Electrochemical studies of manganese tetraaminophthalocyanine monomer and polymer, Electrochim. Acta 49 (2004) 1417–1428.
[24] A. Sivanesan, J.S. Abraham, Amino group position dependent orientation of self-assembled monomolecular films of tetraaminophthalocyanatocobalt(II) on Au surfaces, Langmuir 24 (2008) 2186–2190.
[25] Y.-H. Tse, P. Janda, H. Lam, W.J. Pietro, A.B.P. Lever, Monomeric and polymeric tetraaminophthalocyaninatocobalt(II) modified electrodes: electrocatalytic reduction of oxygen, J. Porphyr. Phthalocyan. 1 (1997) 3–16.
[26] K.L. Brown, J. Shaw, M. Ambrose, H.A. Mattola, Voltammetric, chronocoulometric and spectroelectrochemical studies of electropolymerized films based on Co(III/II)- and Zn(II)-4,9,16,23-tetraaminophthalocyanine: effect of high pH, Microchem. J. 72 (2002) 285–298.
[27] A. Goux, F. Bedioui, L. Robbiola, M. Pontie, Nickel tetraaminophthalocyanine based films for the electrocatalytic activation of dopamine, Electroanalysis 15 (2003) 969–974.
[28] T.F. Otero, E.D. Larreta-Azelain, Electrochemical generation of polythiophene films on platinum electrodes, Polymer 29 (1988) 1522–1527.
[29] M.S. Ureta-Zanartu, A. Alarcon, C. Berrios, G.I. Cardenas-Jiron, J. Zagal, C. Gutierrez, Electropreparation and characterization of polyNiTSPc films. An EQCM study, J. Electroanal. Chem. 580 (2005) 94–104.
[30] T.R.I. Cataldi, D. Centonze, G. Ricciardi, Electrode modification with a poly(NiII-tetramethyldibenzotetraaza[14]annulene) film. Electrochemical behavior and redox catalysis in alkaline solutions. I, Electroanalysis 7 (1995) 312–318.
[31] T.R.I. Cataldi, E. Desimoni, G. Ricciardi, L. Francesco, Study of the nickel-based chemically modified electrode obtained by electrochemical deposition of an NiII-tetramethyldibenzotetraaza[14]annulene complex. Redox catalysis of carbohydrates in alkaline solutions. II, Electroanalysis 7 (1995) 435–441.
[32] S. Trevin, F. Bedioui, M.G. Gomez Villegas, C. Bied-Charreton, Electropolymerized nickel macrocyclic complex-based films: design and electrocatalytic application, J. Mater. Chem. 7 (1997) 923–928.
[33] A.J. Bard, L.R. Faulkner (Eds.), Electrochemical Methods: Fundamentals and Applications, Wiley, New York, 1980.
[34] J.J. Gooding, V.G. Praig, E.A.H. Hall, Platinum-catalyzed enzyme electrodes immobilized on gold using self-assembled layers, Anal. Chem. 70 (1998) 2396–2402.
[35] S. Griveau, V. Albin, T. Pauporte, J.H. Zagal, F. Bedioui, Comparative study of electropolymerized cobalt porphyrin and phthalocyanine based films for the electrochemical activation of thiols, J. Mater. Chem. 12 (2002) 225–232.
[36] P. Westbroek, G. Priniotakis, P. Kiekens, Analytical Electrochemistry in Textiles, Woodhead Publishing Limited and CRC Press LLC, Cambridge, England, 2005.
[37] P.S. Kumar, V. Lakshminarayanan, Electron-transfer studies in a lyotropic columnar hexagonal liquid crystalline medium, Langmuir 23 (2007) 1548–1554.
[38] L. Yang, Y. Li, AFM and impedance spectroscopy characterization of the immobilization of antibodies on indium–tin oxide electrode through self-assembled monolayer of epoxysilane and their capture of Escherichia coli O157:H7, Biosens. Bioelectron. 20 (2005) 1407–1416.
[39] I.A. Akinbulu, T. Nyokong, Characterization of polymeric film of a new manganese phthalocyanine complex octa-substituted with 2-diethylaminoethanethiol, and its use for the electrochemical detection of bentazon, Electrochim. Acta 55 (2009) 37–45.
[40] S. Khene, D.A. Geraldo, C.A. Togo, J. Limson, T. Nyokong, Synthesis, electrochemical characterization of tetra- and octa-substituted dodecyl-mercapto tin phthalocyanines in solution and as self-assembled monolayers, Electrochim. Acta 54 (2008) 183–191.
[41] A.B.P. Lever, E.R. Milaeva, G. Speier, in: C.C. Leznoff, A.B.P. Lever (Eds.), Phthalocyanines: Properties and Applications, vol. 3, VCH Publishers, New York, 1993.
[42] J.C. Miller, J.N. Miller, Statistics for Analytical Chemistry, E. Horwood, Chichester, 1984.